INVESTIGATION OF THE VOLUME LAMP SOURCES OF EMISSION

A.M. Boichenko, R.I. Golyatina, S.A. Maiorov, and S.I. Yakovlenko.

Institute of General Physics
of the Russian Academy of Sciences, Moskow
Received April 15, 1995

Operation of the ArF *and* KrCl *exciplex lamps in* Ne—Ar—F_2 *and* Ne—Kr—HCl *gas mixtures pumped with a glow discharge are investigated theoretically. Optimization of the conditions for these lamp operations is shown to be achievable. The spatial intensity distribution from the lamps of simplest geometry, cylindrical and coaxial, is calculated.*

INTRODUCTION

There are many applications where coherency or high power of output beams is not needed. When laser sources are substituted by lamps (fluorescent sources), it is possible to reduce the requirements to their maintenance and to widen the range of operation parameters. In such a case, atomic and molecular transitions that do not provide lasing are quite suitable. Depending on application, both sources of a narrow-band and broad-bamd emission can be used, as is described in the review.[1]

Rare gas halide exciplex lasers are the most powerful sources of UV and VUV coherent radiation. So it is reasonable to consider exciplex mixtures as the most promising sources of efficient UV and VUV spontaneous emission. Generally speaking, optimal operation modes of a lamp source and a laser are different.

We analyze here three kinds of discharge lamp pumping, i.e., barrier discharge pumping[2,6,13] microwave discharge pumping,[4,5] and volume discharge pumping[1,3,7–9,11,12]. Spatial distribution of the lamp emission intensity has been studied in Refs. 10,11, and 13.

In this paper we consider exciplex lamps pumped by volume discharge as well as output intensity profiles near the lamp with and without amplification in the medium. The effect of energy loading, gas pressure, and mixture composition on the output characteristics of the discharge ArF (He—Ar—F_2 mixture, B–X transition, λ = 193 nm) and KrCl (Ne—Kr—HCl mixture, B–X transition, λ = 222 nm) lamp sources is studied theoretically. No theoretical results on ArF lamp sources pumped by volume discharge are available (experimental data can be found in Refs. 1, 11). Mainly the KrCl lasers and lamps have been studied experimentally. Comparison of KrCl and XeCl lamp operation demonstrates that the KrCl system is less efficient than the XeCl system if HCl molecules are used as a chlorine donor,[1,7,11,13] and these systems have apparently the same efficiency if Cl_2 molecules are used[12] (stationary glow discharge was examined in Refs. 7,12).

A detailed description of ArF and KrCl lamp kinetic model is beyond the scope of this paper. It should be noted that these models were developed using the experience in simulation of the KrF, ArF, XeCl and XeF laser operation.[14–19]

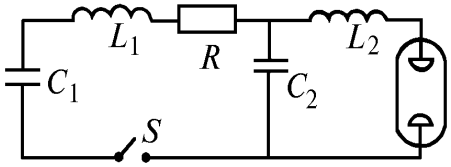

FIG. 1. Electricl circuitry: S is a switch, C_1 = 8 nF, C_2 = 3.4 nF, L_1=30 nH, L_2 = 5 nH, R = 0.17 Ω. *Electrode area is equal to* 50.26 cm^2, *electrode separation is* 2 cm (ArF *lamp*) *and* 3.5 cm (KrCl *lamp*)

The excitation electric circuitry which was included into the model is shown in Fig. 1. A capacitor C_1 is charged to a voltage U, and then a switch is triggered.

ArF LAMP

Our calculations are based on a kinetic model that was used previously[17,18] for simulation of an ArF laser. Output energy and the lamp efficiency relative to the energy deposited increase as the gas pressure decreases down to approximately 170 Torr (N_{He} = $6 \cdot 10^{18}$ cm^{-3}). Optimal concentrations of argon and fluorine remain nearly constant as the total gas pressure is varied (see Fig. 2).

By the emitted energy we understand here the energy emitted within the solid angle $\Omega = 4\pi$. When total gas pressure is decreased down to 42 Torr output energy and efficiency show the same tendency to increase ($\eta \approx 25\%$) but optimal partial pressure of argon and fluorine is different for output energy and efficiency. The highest value of the efficiency is reached at Ar and F_2 concentrations lower than those corresponding to operation at the highest power. It should be mentioned that the highest output energy is reached at the Ar concentration comparable or even

0235-6880/95/11 876-07 $02.00

higher than He concentration. For this reason, Fig. 2 illustrates output energy and efficiency versus gas pressure not lower than 85 Torr. It is not difficult to calculate efficiency based on the energy stored in the capacitor C_1 since the specific output energy is presented in Fig 2 and radiating volume $V = 100.5$ cm^3 as well as the energy stored in the capacitor $E_n = C_1 U_0^2/2 = 3.6$ J are known. This efficiency is about 10% at the He pressure of 85 Torr. It should be noted that no discharge constriction was taken into consideration in our calculations. The constriction is known to limit the output energy and efficiency of a discharge device operating under real conditions even if no halogen depletion is observed.

The curves illustrating the output energy and efficiency as functions of argon and fluorine concentration are very smooth near their optimal values. The less is the total pressure, the more smooth are the curves. This is not an extraordinary situation since collisional quenching of the excited states is less pronounced at low gas pressure. Optimal argon concentration increases from 5–10% at higher gas pressure (2 atm) up to 20–100% at lower gas pressure (≤ 100 Torr) whereas fluorine concentration increases from about 0.1–0.2% up to 1–2% (see the table). Optimal argon and fluorine concentrations obtained in our calculations are in a good agreement with experimental data presented in Ref. 11 obtained at a gas pressure of 1.5–2 atm and under a different initial conditions (d, U_0, circuit parameters). Similarly to lasing behavior, energy of fluorescence increases almost linearly with charging voltage increase.

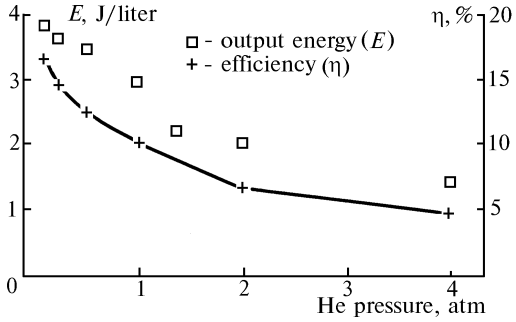

FIG. 2. Total output energy and the efficiency relative to the energy deposited into gas versus gas pressure. Ar *and* F_2 *concentrations are optimized at each value of the gas pressure. Charging voltage is* U_0=30 kV.

TABLE. Optimal concentrations of Ar *and* F_2 (*in* cm^{-3}) *as functions of* He *pressure.*

[He]	3 (18)*	6 (18)	1.35 (19)	2.7 (19)	5.4 (19)	1.08 (20)
$[Ar]_{opt}$	2–0.6 (18)	2–1.35 (18)	2.7–2 (18)	2.7–1.35 (18)	4 –2.7 (18)	4– 2.7 (18)
$[F_2]_{opt}$	0.7–0.35 (17)	0.7–0.35 (17)	1–0.7 (17)	1–0.7 (17)	1.42–1 (17)	1.42–1 (17)

* The order of number is indicated in brackets, for instance, 3 (18) = $3 \cdot 10^{18}$.

The operation of exciplex lamps pumped using the technique considered has been experimentally studied only at gas pressure higher than 1 atm (Refs. 8, 9, 11). Similar conditions of operation took place in Ref. 3 with a KrF lamp. The main regularities observed in this paper well agree with our conclusions. These are optimal lamp operation at a low gas pressure (≤ 100 Torr), higher halogen concentration ($He/Kr/F_2 = 90.5/7.5/2$) as compared with the laser operation and weak dependence of the output energy on [Kr] and [F_2] near their optimal values.

KrCl LAMP

Simulation of a KrCl lamp operation has been done based on the same electric circuitry as in the case with ArF lamp (see Fig. 1), but in contrast to it we have assumed preionization to occur during the rise of the voltage applied to the gasdischarge chamber ($\tau = 40$ ns) at the ionization frequency $\nu = 200$ s^{-1}. KrCl laser is known to operate very bad without the preionization and so we included it into the model of the lamp operation. No discharge constriction was considered in the model.

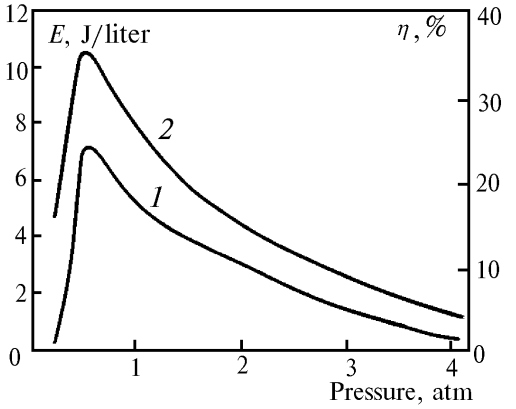

FIG. 3. Total output energy (1) and efficiency relative to the energy loading (2) versus pressure. Kr *and* HCl *concentrations were optimized at each value of the gas pressure,* U_0 = 35 kV.

Optimal pressure falls within the range of 0.5–1 atm at the voltage applied to the capacitor C_1U = 35 kV (see Fig. 3). The preionization energy $E = E_P \nu N \tau V$ is 0.2 J at a gas pressure of 1 atm. E_P is

the energy of formation of one electron-ion pair in Ne. The value of preionization energy is about 4 % of the energy stored in the capacitor. This value is a small fraction of energy deposited into the gas from discharge at optimal gas pressure (< 10%). Figure 3 shows the efficiency of the lamp relative to energy deposited into the active medium from preionization and from the discharge. Time behavior of KrCl (*B*, *C*) concentration is illustrated in Fig. 4.

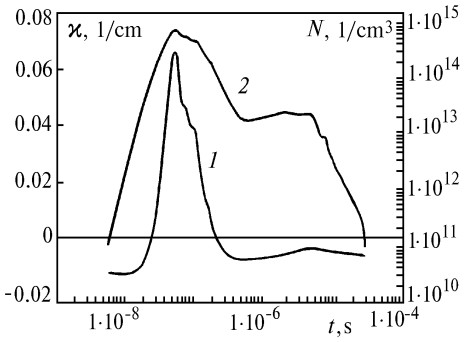

FIG. 4. Time profiles of KrCl *number density (2) and gain* $\varkappa$ *(1),* $\varkappa_0 = \varkappa^+ - \varkappa^-$, *at* [Ne] = $2.7 \cdot 10^{19}$ cm^{-3}, $[k_2] = 4.7 \cdot 10^7$ cm^{-3}, [HCl] = $1.5 \cdot 10^{16}$ cm^{-3}, $U_0 = 35$ kV.

The population of exciplex molecules peaks in a time comparable to the preionization time. Then quasistationary stage of the discharge is observed. Under optimal conditions it lasts from several microseconds to several tens of microseconds, concentration of KrCl molecules being 0.01 of its maximum value. Since its duration is much longer than the stage of high KrCl concentration, the energy emitted during this stage is about two times higher than that emitted during the period corresponding to KrCl concentration being higher than 0.1 of its peak value. The quasistationary stage is observed in the gas pressure range from 0.5 to 1 atm. It is less obvious at $p = 2$ atm being hardly observable at $p = 0.25$ and 4 atm. Under these conditions the energy emitted during this stage is negligibly small.

Optimal value of the efficiency relative to the energy deposited into the medium is close to the quantum efficiency $\eta_{ph} = \hbar\omega / E^* = 5.58/16.6 = 33.6\%$. Here $\hbar\omega$ is the energy of emitted photon, and E^* is the energy of the first excited level of Ne atoms. If the quasistationary stage is absent (for instance, under conditions of insufficient preionization), the efficiency relative to energy deposited into the gas is 10–20%. A possibility of achieving efficiency of ArF lamp close to the quantum limit (≈ 20%) was shown in previous section. Efficiency of about 5% (KrF, Ref. 3) and about 12% (KrCl, XeCl, Ref. 12) was obtained with longitudinal discharge and about 12% (KrF, Ref. 5) was observed with a microwave discharge. It should be pointed out that if the efficiency is calculated using the value of radiation intensity, the measurements are to be made carefully since output intensity falls dramatically with the distance from the lamp.[10,11,13] This may lead to understated value of the lamp efficiency.

In the range of gas pressure inverstigated ($p = 0.25 - 4$ atm), optimal HCl concentration is $1.5–2 \cdot 10^{16}$ cm^{-3} and optimal Kr concentration is approximately $5 \cdot 10^{17}$cm^{-3} at $p = 1–4$ atm, $6 \cdot 10^{17}$ cm^{-3} at $p = 0.5$ atm, and $2 \cdot 10^{18}$ cm^{-3} at $p = 0.25$ atm. At $p = 0.25$ and 4 atm the peak of output energy versus [HCl] is weakly pronounced. At a pressure $p = 0.25$ atm only weak optimum is observed with respect to partial pressure of Kr. Experimental values of Kr and HCl concentrations ($p_{Kr} = 45$ Torr, $p_{HCl} = 2–3$ Torr, Ref. 11) measured at the electrode gap of $d = 2.5$ cm are three times higher than those calculated at $d = 3.5$ cm. Following Ref. 11, optimal pressure (3 atm) is also approximately three times higher than the calculated value.

It should be noted that according to our model, if we fix [Kr] and [HCl] at the values presented in Ref. 11, optimal gas pressure will be about 2 atm. Optimal gas pressure obtained in the experiments performed with a barrier discharge is 1 atm for the same mixture. Fast drop of the output when Kr concentration exceeds 10^{18} cm^{-3} is related to a dramatic reduction of the average electron energy and to the intense Kr^+ formation. The Cl^- ions are mainly produced by electron attachment to HCl ($\nu = 0$) molecules. However, the cross section of this process is at least an order of magnitude smaller than that for vibrational excitation of HCl molecules:

$$HCl\ (\nu = 0) + e \rightarrow HCl\ (\nu = 1) + e.$$

As a result, increase in the initial HCl concentration will lead to lower average electron energy in the discharge. Generally speaking, a decrease in the output energy and efficiency at $[Kr] < [Kr]_{opt}$ and $[HCl] < [HCl]_{opt}$ is connected with halogen depletion whereas the same tendency observed at $[Kr] > [Kr]_{opt}$ and $[HCl] > [HCl]_{opt}$ is related to reduction of the average electron energy and to Kr^+ formation. When [Kr] > 10^{18} cm^{-3} the discharge is nonuniform, and at $t > 6$ μs the discharge voltage is nealy constant at a level of about 23 kV during $t \geq 100$ μs.

MODELING OF OUTPUT FLUX FROM EXCIPLEX LAMPS

In a rather wide class of optical problems there is a possibility to ignore the wave properties of light and to characterize it by the intensity. In this case, both lamps and lasers can be considered as volume emitters. The volume emitters are characterized by the density of emitters distributed over the volume and by absorption (or gain) coefficient of the medium. The intensity of radiation both inside the emitter and outside it is derived by solution of the radiative transfer equation.

In the problem of radiative transfer (see for instance, Refs. 20–22) the light field is often considered as an ensemble of photons. The field is entirely described by the corresponding distribution function $f(t, \mathbf{r}, \mathbf{n}_\Omega)$, $f(t, \mathbf{r}, \mathbf{n}_\Omega)d\omega\, dV\, d\Omega$ being the number of photons with a frequency in the range $(\omega, \omega + d\omega)$ at a time moment t in the volume dV at a point $\mathbf{r}$ within a solid angle $d\Omega$ about a unit vector $\mathbf{n}_\Omega$ along the direction of movement. However, in the theory of radiative transfer the light field is usually characterized not by photon distribution function but by spectral intensity that is expressed as follows:

$$I_\omega(t, \mathbf{r}, \mathbf{n}_\Omega) = \hbar\omega c\, f(t, \mathbf{r}, \mathbf{n}_\Omega) \quad [\mathrm{W}/(\mathrm{cm}^2\cdot\mathrm{sr})] .$$

The light field is characterized also by radiation density U_ω, i.e. by the quantity of radiative energy within a unit volume. It can be expressed as follows:

$$U_\omega(t, \mathbf{r}) = \hbar\omega \int_{4\pi} f_\omega(t, \mathbf{r}, \mathbf{n}_\Omega)\, d\Omega =$$

$$= \frac{1}{c} \int_{4\pi} I_\omega(t, \mathbf{r}, \mathbf{n}_\Omega)\, d\omega \ [\mathrm{J}/\mathrm{cm}^3] .$$

Besides, it is characterized by the vector of radiation flux density that can be expressed in the following form:

$$J_\omega(t, \mathbf{r}) = \int_{4\pi} \mathbf{n}_\Omega\, I_\omega(t, \mathbf{r}, \mathbf{n}_\Omega)\, d\Omega \ [\mathrm{W}/\mathrm{cm}^2].$$

Its projection onto a selected direction $\mathbf{n}$ is conventionally defined as the radiation flux[20]:

$$J_\omega(t, \mathbf{r}) = \int_{4\pi} I_\omega(t, \mathbf{r}, \mathbf{n}_\Omega) \cos(\hat{\mathbf{n}\mathbf{n}_\Omega})\, d\Omega .$$

In this equation, $\hat{\mathbf{n}\mathbf{n}_\Omega}$ denotes angle between vectors $\mathbf{n}$ and $\mathbf{n}_\Omega$. As a rule, vector $\mathbf{n}$ determines orientation of a surface element dS of a photodetector.

Consider next two integral characteristics, the radiation flux and its density, on a screen of photodetectors oriented in a certain way.

The spatiotemporal intensity variations are described by equation of radiative transfer[20–22]:

$$\frac{dI_\omega}{dt} = \frac{\partial I_\omega}{\partial t} + c\, \mathbf{n}_\Omega \frac{dI_\omega}{d\mathbf{r}} = c\, \varkappa(\omega)\, I_\omega + \frac{c}{4\pi} Q_\omega ,$$

Here $\varkappa(\omega)$ is the gain (absorption) coefficient; Q_ω is the power of spontaneous emission with the spectrum falling within a range from ω to $\omega + d\omega$ per unit volume of the medium with the center at the point $\mathbf{r}$. In the general case, $\varkappa$ can be positive or negative and can depend on I_ω. Local optical characteristics of the medium $\varkappa(\omega)$ and Q_ω are normally found by solution of corresponding kinetic (relaxation) equations (see, for instance, Ref. 23).

When excilamps with $\varkappa L \le 1$ (the opposite is valid for the laser media where $\varkappa L \gg 1$) are considered, distortions of optical characteristics due to absorption and amplification in the medium can be neglected.In this case, index ω in designations of optical characteristics can be omitted. Besides, let us consider stationary equation of radiative transfer:

$$\mathbf{n}_\Omega\, \partial I/\partial \mathbf{r} = \varkappa I + (1/4\pi) Q .$$

The calculations have been performed according to the following scheme. A region involving both emitting volume and surfaces that determine photodetector screens is considered. Tests of the total number n are carried out, and all of them are characterized by production of a photon in the emitting volume. Probability of photon production at one or another point of the space $\mathbf{r}$ depends on spontaneous emission source density distribution $Q(\mathbf{r})$. Photon can be emitted in any direction with equal probability.

Then the photon is followed up till it leaves the region considered or falls on a photodetector. First consider the case when both amplification and absorption of photons in the medium are absent ($\varkappa = 0$). In this case, number of photons $n_\Delta(\mathbf{r})$ passing through an element of a photodetector surface $\Delta\sigma$ close to a point $\mathbf{r}$ is in direct proportion to the flux J if number of tests n is sufficiently large, and we have

$$J(\mathbf{r}) = \dot{E}\, w_J(\mathbf{r}) , \qquad w_J(\mathbf{r}) = n_\Delta(\mathbf{r})/(\Delta\sigma n) . \qquad (1)$$

The proportionality coefficient is expressed as

$$\dot{E} = \int_{(V)} Q(\mathbf{r})\, dV,$$

and it is related to the energy emitted by the volume in a unit time interval; $w_J(\mathbf{r})$ is the probability of a photon to pass through a unit cross section of the photodetector screen in the vicinity of a point $\mathbf{r}$.

To obtain volume radiation density $U(\mathbf{r})$, it is necessary to calculate the time of a photon staying in a cell in the vicinity of the point $\mathbf{r}$ (compare with Ref. 24). If we are interested in the values of radiation density at the points close to photodetector, we have for the time of jth photon staying that passes a volume with thickness Δl over an area $\Delta\sigma$:

$$\Delta t_j = (\Delta l/c)/\cos\vartheta_j .$$

Here ϑ_j is the angle between the direction of photon propagation and normal to the area $\Delta\sigma$. Thus,

$$U(\mathbf{r}) = (\dot{E}/c)\, w_U(\mathbf{r}),$$

$$w_U(\mathbf{r}) = (1/\Delta\sigma n) \sum_{j=1}^{n_\Delta} (\gamma_j^0/\cos\vartheta_j) , \qquad (2)$$

w_U is the probability of a photon detection in the vicinity of a unit surface and the point **r** of the screen. It is evident that the values w_J and w_U do not coincide.

So, our calculations give values E, w_J and w_U. Other quantities can be easily experessed in terms of these three parameters.

Absorption or amplification of jth photon is taken into account according to the following equation:

$$\gamma_j = \gamma_j^0 \exp\left(\int_{S_j}^{S_{1j}} \varkappa\, ds\right).$$

The integration is done here over the ray from the point S_j of a photon production to the point S_{1j} where it leaves the emitting volume.

Then, the definition of probabilities in Eqs. (1) and (2) is changed:

$$w_J(\mathbf{r}) = (1/\Delta\sigma n) \sum_{j=1}^{n_\Delta} \gamma_j ,$$

$$w_U(\mathbf{r}) = (1/\Delta\sigma n) \sum_{j=1}^{n_\Delta} \gamma_j/\cos\vartheta_j .$$

SIMULATION OF A CYLINDRICAL LAMP

We consider here the case with uniform emitters with $Q(\mathbf{r}) = Q_0 = \text{const}$. Then, the presence of amplification in the mediun is assumed. As it should be expected, in this case an increase in the flux and radiation density with gain in the medium is slower at the center of the emitting region than at its boundaries. Indeed, our calculations confirm this conclusion (see Fig. 5). Moreover, it is seen that behavior of the flux and radiation density is different as the amplification of the medium increases.

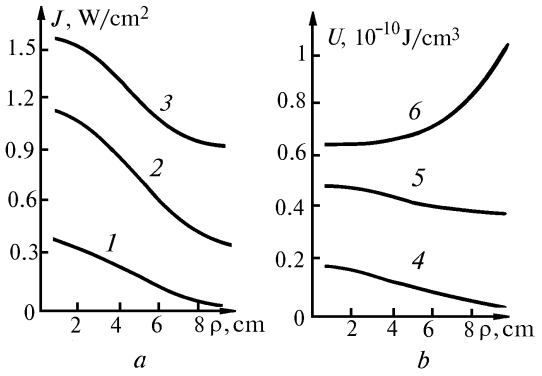

FIG. 5. Spatial distribution of radiative flux (a) and volume radiation density (b) over the radius in a plane normal to the axis of a cylindric lamp: L = 2 cm, z = 2 cm, R = 4 cm, Q_0 = 1 W/cm^3; $\varkappa$ = 0 (curves 1,4), 0.8 (curves 2,5), and 1 (curves 3,6).

It should be noted that an analytical expression for U at $\varkappa = 0$ has been derived in Ref. 10,11. For a flat screen located normally to a cylinder of length L and radius R at a distance z from the nearest end of the cylinder we have (Fig. 5, curve *4*):

$$\begin{aligned}
U(\rho) = (Q_0/4\pi c) \Big\{ & \pi(z+L)\, \ln\{[(z+L)^2 + \\
& + \rho^2 + R^2]/[(z+L)^2 + \rho^2]\} - \\
& - \pi z\, \ln[(z^2 + \rho^2 + R^2)/(z^2 + \rho^2)] + 2\pi(\rho^2 + R^2)^{1/2} \times \\
& \times \arctan[(z+x)/(\rho^2 + R^2)^{1/2}]\Big|_{x=0}^{x=L} - \\
& - 2\pi\rho\, \arctan[(z+x)/\rho]\Big|_{x=0}^{x=L} + \\
& + \pi \sum_{n=1}^{\infty} [(2n-1)!!/2^n n!] \times \\
& \times (2\rho)^{2n} \sum_{k=0}^{n} \binom{n}{k} [(-1)^{n-k}/(2n-k)] \times \\
& \times \Big[A_1(n, \rho, z+x)\Big|_{x=0}^{x=L} - \\
& - \rho^{2(n-k)}\, A_1(2n-k, (\rho^2 + R^2)^{1/2}, z+x)\Big|_{x=0}^{x=L} - \\
& - \sum_{m=1}^{n-k} \binom{n-k}{m} \rho^{2(n-k-m)} \times \\
& \times A_2(m, 2n-k, (\rho^2 + R^2)^{1/2}, z+x)\Big|_{x=0}^{x=L} \Big] \Big\} ,
\end{aligned} \tag{3}$$

where

$$A_1(n, \rho, x) = \int_0^x dy/(y^2 + \rho^2)^n;$$

$$A_2(m, n, \rho, x) = \int_0^x y^{2m}\, dy/(y^2 + \rho^2)^n$$

Here ρ is the distance between the point where the axis of the cylinder intersect the screen and the point of a photon incidence.

COAXIAL LAMP

Coaxial lamps with reflecting inner surface are of a certain interest in some application. In this case, it is reasonable to consider coaxial geometry of a photodetector screen. Calculation of the radiation density emitted from a coaxial lamp in the absence of amplification has been performed earlier[13] using characteristics of radiation scattering on a cylinder.

Let us derive expression for the radiative flux from an infinite coaxial lamp with no amplification through a coaxial photodetector screen. This will be the estimation from above of the flux from a lamp of finite length.

Let R be outer radius of the lamp, R_0 be the radius of the inner cylinder with the reflection coefficient k, R_s is the radius of a photodetector. The case of $R_0 = 0$ corresponds to conventional cylindric lamp. Energy flux through a cylindric screen in the case of a infinite uniform cylinder can be written as:

$$J_\infty = Q_0 R^2/2R_S .$$

The probability of a photon absorption by the inner cylinder of a infinite coaxial lamp is

$$W_p = (1 - k)/(\pi(R^2 - R_0^2)) \int_{R_0}^{R} 2r \arcsin(R_0/r)\, dr .$$

If the integral in this equation is denoted as S_0 we have:

$$S_0 = R^2 \arcsin(R_0/R) + R_0 \sqrt{R^2 - R_0^2} - \pi R_0^2/2.$$

Probability for a photon to reach the screen is determined by the following expression:

$$W_F = 1 - W_p = 1 - (1 - k)\, S_0/(\pi(R^2 - R_0^2)) .$$

Taking into account the fact that the number of particles produced in a coaxial lamp related to that in a uniform cylinder is equal to the ratio of emitting volumes, we obtain an expression for the energy flux J_k through a distant coaxial screen to be as follows

$$J_k = J_\infty W_F (R^2 - R_0^2)/R^2.$$

As we have already mentioned, radiation density coming from a coaxial lamp with no amplification has been calculated previously[13]. The values of density at $k = 0.5$ and 1 seem to be slightly overestimated in Ref. 13 (not more than by 10%). Other data agree with those obtained by the Monte Carlo method.

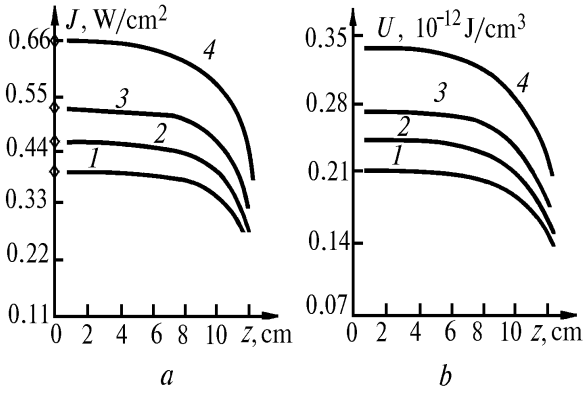

FIG. 6. Spatial distribution of radiative flux (a) and volume radiation density (b) over the length of a coaxial screen z for coaxial geometry of the lamp z = 0 corresponds to the center of emitting volume: L = 25 cm, R = 1.7 cm, R_0 = 0.8 cm, R_S = 2.2 cm, $\varkappa$ = 0, Q_0 =1 W/cm^3; k = 0 (curve 1), k = 0.5 (curve 2), k = 1 (curve 3) and curve 4 corresponds to a uniform cylinder. Markers on the axes Y indicate values of the flux J_k obtained with infinite lamp in the absence of amplification.

Behaviors of J and U parameters as functions of different variables (for instance, distance from the lamp axis l and distance from the lamp center in longitudinal direction z at a fixed l) are similar (see Fig. 6 and experimental data on $U(l)$ presented in Ref. 13). When amplification is present in the medium increase in J and U with $\varkappa$ is more pronounced at the ends than at the center, similarly to previous case.

CONCLUSION

Optimal regimes of operation for a ArF and a KrCl lamp with He—Ar—F_2 and Ne—Kr—HCl gas mixtures pumped by volume discharge have been shown to exist by calculations. Unlike the KrF lamp[3] and ArF lamp with mixtures containing F_2, optimal pressure in KrCl lamp is not low (0.5—1 atm) whereas neither absolute nor relative value of optimal HCl concentration exceeds that in the lasing regime. This is caused by specific features of HCl molecules. When the pressure of fluorine-containing gas mixture is decreased, three-body ion—ion recombination that serves as the main mechanism of exciplex formation is gradually replaced by harpoon reactions. That is why the optimal value of the initial F_2 concentration is to be increased at a low pressure. This is not valid for HCl-containing mixtures, since an increase in the initial HCl concentration results in an efficient electron cooling and slower formation of the excited krypton atoms. When a preionized Ne—Kr—HCl gas mixture is pumped by a discharge, the quasistationary stage of excitation whose duration can reach several tens of microseconds can occur. This stage provides an appreciable output of radiation.

The problem of calculating flux density and radiation density from a lamp source with an arbitrary emitting region, arbitrary gain distrubution over the emitting region, and an arbitrary location of reflecting surfaces has been numerically solved in geometric-optics approximation. It is natural that the Monte Carlo method is used for these calculations. Such an approach has a number of advantages since it is difficult to derive analytical expressions and even if such expressions are obtained they can be processed only numerically.

A dramatic drop of J and U values has been discovered to occur at the distance equal to characteristic minimum dimension of the emitting volume. At relatively short distances, J and U profiles are similar in the case of the medium with no amplification.

Amplification in the medium causes a significant modification of J and U spatial behavior. Thus, variation of power loading together with geometry of the emitting region strongly influences the spatial dependences of the flux density and radiation density.

REFERENCES

1. A. M. Boichenko, V.F. Tarasenko, E.A. Fomin, and S.I. Yakovlenko, Kvant. Elektron. **20**, 7 (1993); A. M. Boichenko, V.I. Derzhiev, A.A. Kuznetsov, et. al, Trudy IOFAN **42**, 3 (1993).

2. B. Eliasson and U. Kogelschatz, Appl.Phys. **B 46**, 299 (1988).
3. H. Kumagai and M. Obara, IEEE Trans. on Plasma Sci. **16**, 453 (1988).
4. H. Kumagai and M. Obara, Appl. Phys. Lett. **54**, 1583 (1989).
5. H. Kumagai and M. Obara, Appl. Phys. Lett. **54**, 2619 (1989).
6. B. Gellert and U. Kogelschatz, Appl. Phys. **B 52**, 14 (1991).
7. R.S. Taylor, K.E. Leopold, and K.O. Tan, Appl. Phys. Lett. **59**, 525 (1991).
8. B.A. Koval', V.S. Skakun, V.F. Tarasenko, E.A. Fomin, and E.A. Yankelevich, Prib. Tekh. Eksp., No. 4, 244 (1992).
9. B.A. Koval', V.S. Skakun, V.F. Tarasenko, and E.A. Fomin, Pis'ma Zh. Tekh. Fiz., No. 13, 1 (1993).
10. A.M. Boichenko, V.S. Skakun, V.F. Tarasenko, E.A. Fomin, and S.I. Yakovlenko, Kvant. Elektron. **20**, 613 (1993).
11. A.M. Boichenko, V.S. Skakun, V.F. Tarasenko, E.A. Fomin, and S.I. Yakovlenko, Las. Phys. **3**, 838 (1993).
12. A.P. Golovitskii and S.N. Kan, Opt. Spektroskop. **75**, 604 (1993).
13. A.M. Boichenko, V.S. Skakun, V.F. Tarasenko, E.A. Fomin, and S.I. Yakovlenko, Las. Phys. **4**, 635(1994).
14. S.I. Yakovlenko, ed., Trudy IOFAN **21** (1989).
15. A.M. Boichenko, V.I. Derzhiev, A.G. Zhidkov, and S.I. Yakovlenko, Kvant. Elektron. **16**, 278 (1989).
16. A.M. Boichenko, V.I. Derzhiev, A.G. Zhidkov, and S.I. Yakovlenko, Kratk. Soobshch. Fiz., No. 9, 9 (1990).
17. A.M. Boichenko, V.I. Derzhiev, A.G. Zhidkov, and S.I. Yakovlenko, Kvant. Elektron. **19**, 486 (1992).
18. A.M. Boichenko, V.I. Derzhiev, and S.I. Yakovlenko, Las. Phys. **2**, 210 (1992).
19. A.M. Boichenko, A.V. Karelin, and S.I. Yakovlenko, Las. Phys. **5**, No 1, 80 (1995).
20. A. Unzold, *Physics of Stars' Atmospheres* (Forein Literature, Moscow, 1949), 631 pp.
21. Ya.B. Zel'dovich and Yu.P. Raizer, *Physics of Shock Waves and High-Temperature Hydrodynamic Phenomena* (Nauka, Moscow, 1966), 686 pp.
22. S.I. Yakovlenko, *Radiative-Collisional Phenomena* (Energoatomizdat, Moscow, 1984), 208 pp.
23. S.I. Yakovlenko, Las. Phys. **1**, 565–589 (1991).
24. S.A. Maiorov, A.N. Tkachev, and S.I. Yakovlenko, Preprint No. 16, Institute of General Physics of the Russian Academy of Sciences, Moscow (1993).